

## Targeting the vital non-structural proteins (NSP12, NSP7, NSP8 and NSP3) from SARS-CoV-2 and inhibition of RNA polymerase by natural bioactive compound naringenin as a promising drug candidate against COVID-19

Elahe Alebrahim-Dehkordi<sup>a,b,c,\*</sup>, Hamed Ghoshouni<sup>d</sup>, Pooneh Koochaki<sup>e</sup>,  
Mohsen Esmaili-Dehkordi<sup>f</sup>, Elham Alebrahim<sup>g</sup>, Fatemeh Chichagi<sup>h</sup>, Ali Jafari<sup>b,i,j</sup>,  
Sara Hanaei<sup>k,l</sup>, Ehsan Heidari-Soureshjani<sup>m,n</sup>, Nima Rezaei<sup>k,l,o,\*</sup>

<sup>a</sup> Systematic Review and Meta-analysis Expert Group (SRMEG), Universal Scientific Education and Research Network (USERN), Tehran, Iran

<sup>b</sup> Nutritional Health Team (NHT), Universal Scientific Education and Research Network (USERN), Tehran, Iran

<sup>c</sup> Medical Plants Research Center, Basic Health Sciences Institute, Shahrekord University of Medical Sciences, Shahrekord, Iran

<sup>d</sup> Medical student, Faculty of Medicine, Shahid Sadoughi University of Medical Sciences, Yazd, Iran

<sup>e</sup> Department of Cancer Biology, Lerner Research Institute, Cleveland Clinic, Cleveland, OH, USA

<sup>f</sup> Pharmacologist, Shahrekord, Iran

<sup>g</sup> PhD Student in Food Sciences and Engineering, Islamic Azad University, Tehran North Branch, Tehran, Iran

<sup>h</sup> Research Development Center, Sina Hospital, Tehran University of Medical Science, Tehran, Iran

<sup>i</sup> Student Research Committee, Department of Nutrition, School of Health, Golestan University of Medical Sciences, Gorgan, Iran

<sup>j</sup> Golestan Research Center of Gastroenterology and Hepatology, Golestan University of Medical Sciences, Gorgan, Iran

<sup>k</sup> School of Medicine, Tehran University of Medical Sciences, Tehran, Iran

<sup>l</sup> Network of Immunity in Infection, Malignancy and Autoimmunity (NIIMA), Universal Scientific Education and Research Network (USERN), Tehran, Iran

<sup>m</sup> Department of Biology, Faculty of Science, Shahrekord University, Shahrekord, P. O. Box. 115, Iran

<sup>n</sup> Central Laboratory, Shahrekord University, Shahrekord, Iran

<sup>o</sup> Research Center for Immunodeficiencies, Children's Medical Center, Tehran University of Medical Sciences, Tehran, Iran

### ARTICLE INFO

#### Keywords:

Non-structural proteins  
SARS-CoV-2  
COVID-19  
RNA polymerase  
Naringenin  
Remdesivir

### ABSTRACT

The prevalence of SARS-CoV-2-induced respiratory infections is now a major challenge worldwide. There is currently no specific antiviral drug to prevent or treat this disease. Infection with COVID-19 seriously needs to find effective therapeutic agents. In the present study, naringenin, as a potential inhibitor candidate for RNA Polymerase SARS-CoV-2 was compared with remdesivir (FDA-approved drug) and GS-441,524 (Derivative of the drug remdesivir) by screening with wild-type and mutant SARS-CoV-2 NSP12 (NSP7-NSP8) and NSP3 interfaces, then complexes were simulated by molecular dynamics (MD) simulations to gain their stabilities. The docking results displayed scores of -3.45 kcal/mol and -4.32 kcal/mol against NSP12 and NSP3, respectively. Our results showed that naringenin had  $\Delta G$  values more negative than the  $\Delta G$  values of Remdesivir (RDV) and GS-441,524. Hence, naringenin was considered to be a potential inhibitor. Also, the number of hydrogen bonds of naringenin with NSP3 and later NSP12 are more than Remdesivir and its derivative. In this research, Mean root mean square deviation (RMSD) values of NSP3 and NSP12 with naringenin ligand ( $5.55 \pm 1.58$  nm to  $3.45 \pm 0.56$  nm and  $0.238 \pm 0.01$  to  $0.242 \pm 0.021$  nm, respectively) showed stability in the presence of ligand. The root mean square fluctuations (RMSF) values of NSP3 and NSP12 amino acid units in the presence of naringenin were  $1.5 \pm 0.31$  nm and  $0.118 \pm 0.058$ , respectively. Pharmacokinetic properties and prediction of absorption, distribution, metabolism, excretion, and toxicity (ADMET) properties of naringenin and RDV showed that these two compounds had no potential cytotoxicity.

\* Corresponding authors at: Mailing address: Children's Medical Center Hospital, Dr. Qarib St, Keshavarz Blvd, Tehran 14194, Iran.

E-mail addresses: [elahe.alebrahim@gmail.com](mailto:elahe.alebrahim@gmail.com) (E. Alebrahim-Dehkordi), [rezaei\\_nima@tums.ac.ir](mailto:rezaei_nima@tums.ac.ir) (N. Rezaei).

<https://doi.org/10.1016/j.molstruc.2023.135642>

Received 24 April 2022; Received in revised form 16 April 2023; Accepted 21 April 2023

Available online 26 April 2023

0022-2860/© 2023 Elsevier B.V. All rights reserved.

## 1. Introduction

In December 2019, a new coronavirus called the 2019 novel coronavirus (2019-nCoV) or the severe acute respiratory syndrome coronavirus 2 (SARS-CoV-2), caused the onset of pneumonia from China's Wuhan Seafood Market, which spread across China [1,2]. The binding of coronaviruses to specific receptors at the level of host cells is one of the most important determinants of prevalence, pathology and the range of host diversity for the virus [3,4]. These receptors are also one of the most crucial targets for developing antiviral drugs and vaccines [5,6]. There is currently no specific treatment for SARS-CoV-2 infection, so the discovery of new drugs for the treatment of COVID-19 has great importance. The measurements were limited to generate preventive and supportive treatments [7]. Various strategies have been adopted around the world to develop effective drugs for the treatment and prevention of disease progression in patients with COVID-19 [8–11]. Some preliminary studies which applied antiviral drugs in two emerging epidemic coronavirus diseases Middle East Respiratory Syndrome (MERS) and Severe acute respiratory syndrome (SARS) were the basis of some novel studies on SARS-CoV-2 disease. These studies investigated some antiviral therapies that critically blocked human CoVs pathogenic processes viz. neuraminidase inhibitors, nucleoside analogues, and remdesivir [12,13]. The viral genome replication is one of the most crucial processes in the life cycle of SARS-CoV-2, which polymerizes RNA and employs variety of viruses and host proteins [14]. SARS, MERS, and SARS-CoV-2, have 16 non-structural proteins (NSPs), which are encoded by 1a and 1b open reading frames (ORF 1a/1b) [15]. NSPs are conserved in the replication and transcription of various coronaviruses [16–18]. One of the preserved NSP in coronaviruses is NSP 12 which has a “cupped right hand” structure. NSP12 subdomains include finger, palm, thumb, and N-terminal domains, with a total length of 932 amino acids [19–23]. The NSP12 N-terminal domain is a nucleotidyltransferase (NiRAN). This domain is associated with the *Nidovirales* RNA-dependent RNA polymerase (RdR) performance [20], and so SARS-CoV Viral growth is dependent on the NiRAN domain [14]. Some studies have proved that the NiRAN domain of SARS-CoV-2 Nsp12 displays structural features of kinase-like folds [14,20]. The structural analysis of NSP8

showed that it formed a complex with NSP7 during its primer-dependent RdR activity [24–26]. NSP7 and NSP8 are identified as SARS-CoV NSP12 adjuncts that form an essential complex for SARS-CoV replication and stimulate the polymerase activity of NSP12 [20,25]. NSP12 binds to NSP7 and NSP8 and produces a kinase-like folding of SARS-CoV [20] (Fig. 1). Phenolic compounds establish one of the significant classes of auxiliary metabolites in plants. Flavonoids are the main phenolic compounds contained in natural medicines [27–29]. One of the flavanones is Naringenin, the aglycone of Naringin, which is mainly contained in *Citrus* species with numerous pharmacological activities (Fig. 2). Naringenin bioactive effects on humans consists of antioxidant, free radical scavenger, anti-inflammatory, carbohydrate metabolism promoter, and immune system modulator [30,31] (Fig. 2). In the present study, naringenin was selected as a potential inhibitor candidate for RNA Polymerase SARS-CoV-2 and its *in silico* effect compared with remdesivir and GS-441,524.

## 2. Results and discussion

### 2.1. Molecular docking

In this study, naringenin flavonoid, RDV, and GS-441,524 obtained from Pubchem databases were virtually screened against the SARS-CoV-2 RNA-dependent RNA polymerase (NSP12) and SARS-CoV-2 macrodomain RNA polymerase (NSP3). AutoDock results represent the docking scores as Gibbs free energy of binding ( $\Delta G$  kcal/mol). The docking scores of naringenin flavonoid, Remdesivir, and GS-441,524 against both NSP12 and NSP3 are provided in (Table 1). The control drug molecule RDV was shown to gain docking scores of  $-3.45$  kcal/mol and  $-4.32$  kcal/mol against NSP12 and NSP3, respectively. The dissociation constant for protein-ligand binding (EIC or estimated inhibition constant) was calculated for all studied compounds and RDV and the data are presented in (Table 1). Compared to RDV, naringenin showed lower EIC values, with  $131.52 \mu\text{M}$  and  $2.99 \mu\text{M}$  for NSP12 and NSP3, respectively. (Table 2) shows how the studied compounds interact with NSP12 and NSP3. The current investigation focused on the primary RNA Polymerase SARS-CoV-2, particularly NSP12 (NSP7, 8) and NSP3, as

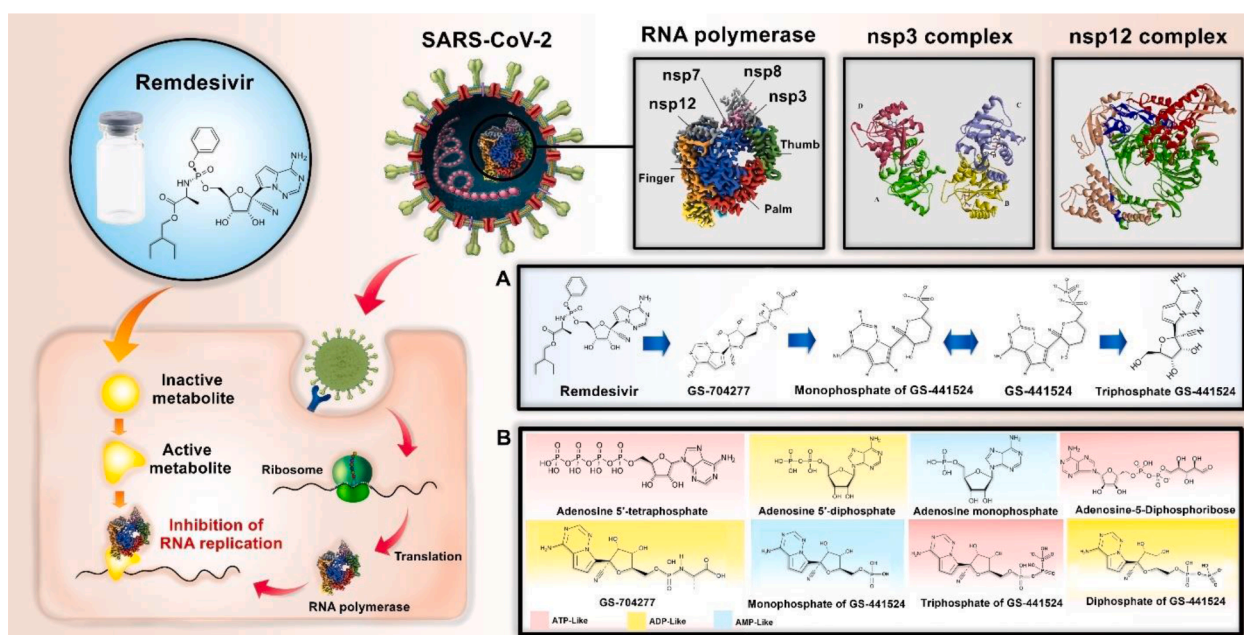


**Fig. 1.** Structure of complex SARS-CoV NSP12 bound to NSP7 and NSP8 co-factors: A Diagram of the SARS-CoV NSP7, 8, and 12 proteins, including conserved motifs, and the protein regions. A. The Metabolism pathway of remdesivir (prodrug) conversion into GS-441,524 (metabolite). B. Structures of ATP, ADP, and AMP-like (size) compounds also display. We observe that the structures of AMP (complex of NSP3) and GS-441,524 monophosphate (complex of NSP12) are highly similar. The size of ADP-ribose (complex of NSP3) and the GS-441,524- triphosphate are resembles.

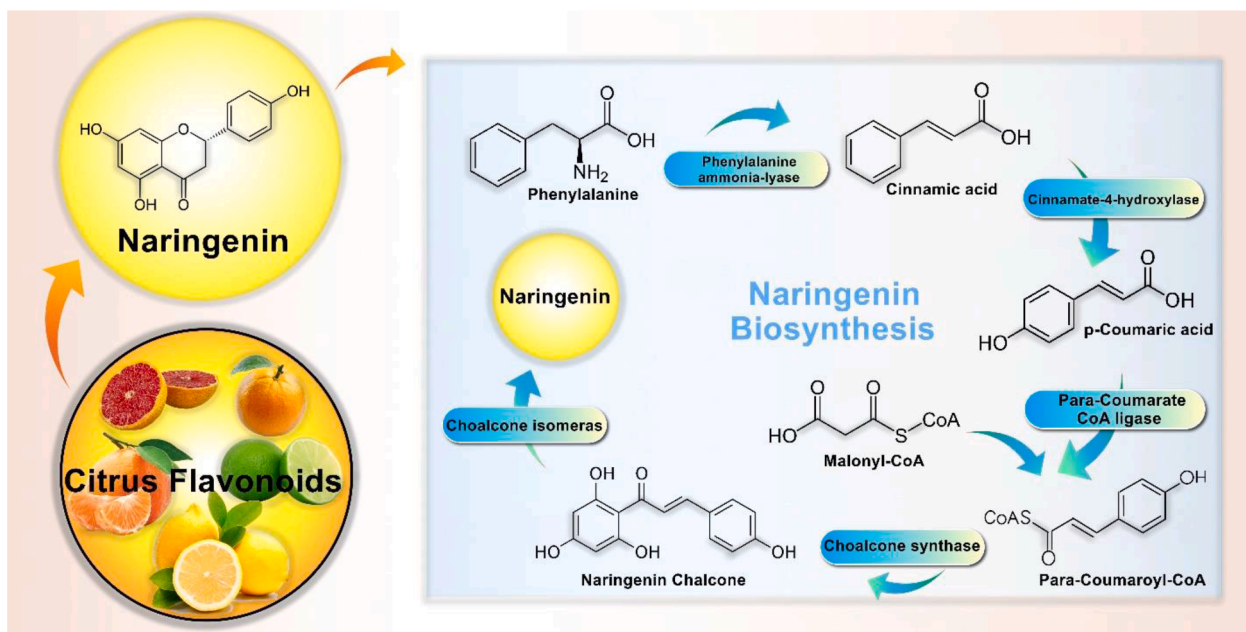


**Fig. 2. Naringenin biosynthesis:** Naringenin is a citrus flavonoid chemically named as 2,3-dihydro-5,7-dihydroxy-2-(4 hydroxyphenyl)-4H-1-benzopyran-4-one. Naringenin distributed molecules are insoluble in water and are soluble in organic solvents, like alcohol. According to the flavonoids class, naringenin is classified as a flavanone, which derives from naringin or narirutin (its glycone precursor) hydrolysis. In fact, Naringenin occupies a central position as primary  $C_{15}$  intermediate in the flavonoid biosynthesis pathway. Overall, the metabolic pathway begins with phenylalanine ammonia-lyase (PAL). Naringenin is produced by the combination of the para-coumaroyl-CoA with three units of malonyl-CoA. Subsequently, para-coumaroyl-CoA is activated by CoA-dependent ligase in the universal phenylpropanoid pathway.

**Table 1**

Docking results in the form of naringenin Binding Affinity used *in silico* screening against SARS-CoV-2 RNA-dependent RNA polymerase (NSP12) and SARS-CoV-2 macrodomain RNA polymerase (NSP3) (AutoDock scores are in kcal/mol).

Receptor/ Protein	Ligand- receptor	BE kcal/ mol	FIE kcal/ mol	EIC $\mu$ M	Interaction bonds Hydrogen Bonding	Hydrophobic Binding	Other Binding
NSP12	Naringenin	-5.29	-6.49	131.52 $\mu$ M	Gln(C)31, Ser(C)60	Ile(D)119, Met(C)62, Pro(D)116, Asn(D)118, Gln(C)63, Val(D)115	Leu(C)28, Val(C)58
	GS-441524	-4.81	-6.60	300.11 $\mu$ M	Cys(A)395, Asp(A)395, Asp(A)390, Ser(A)397, Lys(A)391	Tyr(B)149, Leu(A)388, Leu(A)389, Phe(A)396, Thr(A)393, Thr(A)394	
	Remdesivir	-3.45	-8.52	2.98 mM	Gly(A)852	Ile(A)856, Leu(A)891, Thr(A)853, Thr(A)850, Lys(A)849	Leu(A)895, Asp(A)851
NSP3	Naringenin	-7.54	-8.73	2.99 $\mu$ M	Leu(C)126, Ala(C)129, Ser(C)128, Asn(C)40	Phe(B)156, Val(B)449, Gly(B)48, Gly(B)46, Phe(B)132, Ala(B)39, Ala(B)38, Leu(B)127, Pro(B)125, Gly(B)130	Ile(B)131
	GS-441524	-6.15	-7.93	31.31 $\mu$ M	Asp(C)22, Leu(C)126, Phe(C)156	Ala(C)129, Gly(C)130, Val(C)24, Ala(C)52, Gly(C)48, Pro(C)125, Ala(C)154, Val(C)155, Asp(C)157, Leu(C)160	Ile(C)23, Val(C)49
	Remdesivir	-4.32	-9.39	677.31 $\mu$ M	Asn(D)59, His(D)45	Asn(D)54, Gln(D)62, Tyr(D)42, Asp(D)66	Lys(D)44

**Abbreviations:** BE; Estimated Free Energy of binding (kcal/mol), FIE; final intermolecular energy (kcal/mol), EIC; estimated inhibition constant ( $\mu$ M/mM).

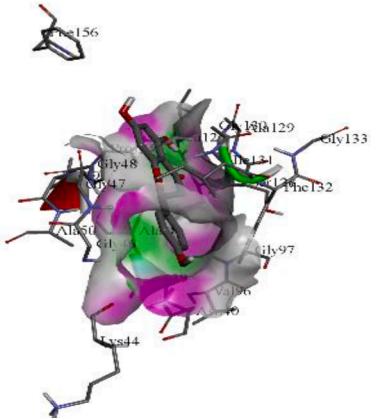
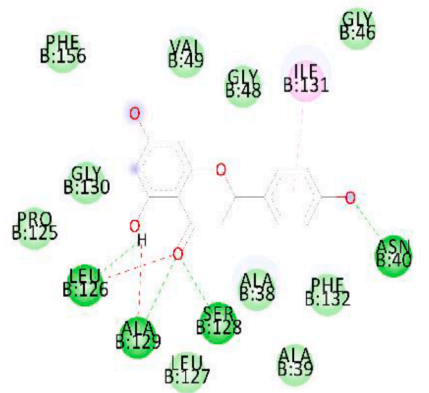
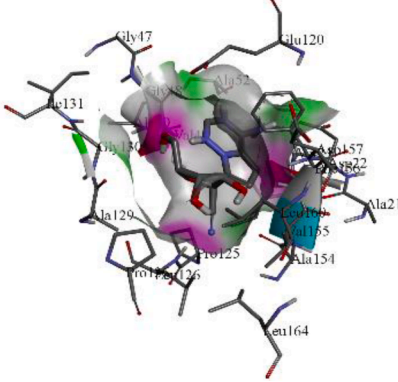
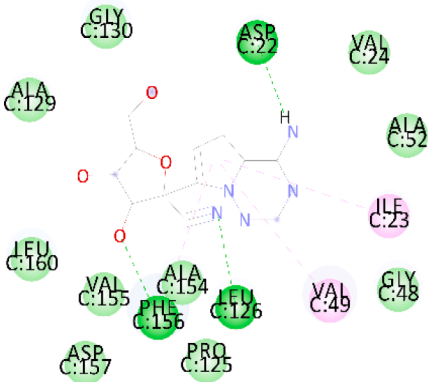
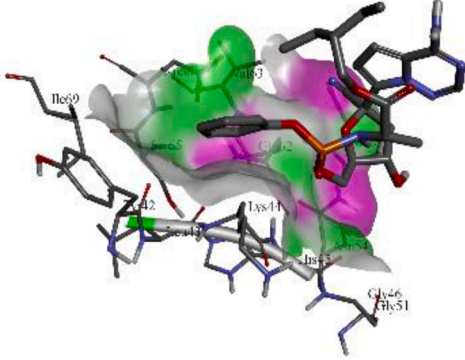
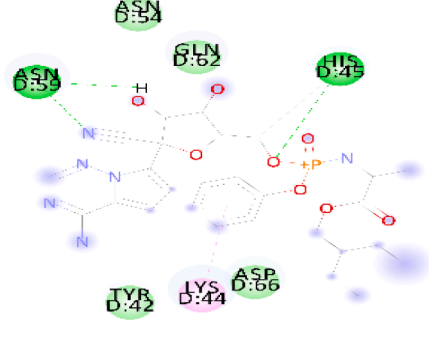
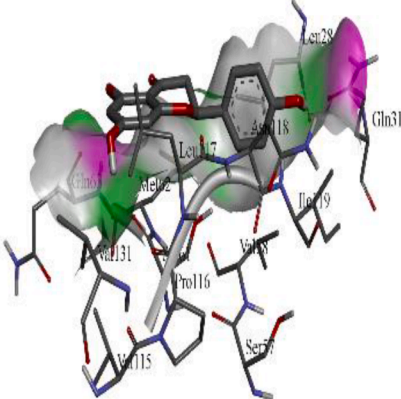
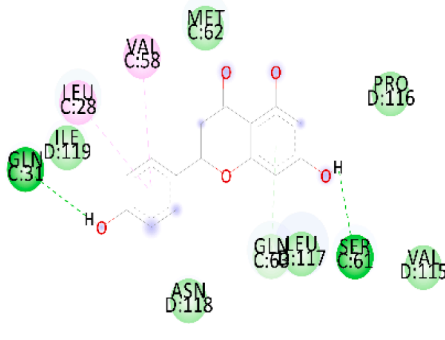
potential objective proteins for COVID-19 treatment. The disclosure of the RNA Polymerase structure in COVID-19 gives an incredible chance to recognize potential medication contenders for treatment. The antiviral impacts of Remdesivir against CoV have been concentrated “in vitro”, in cells contaminated with SARS-CoV [32,33].

Recently, the crystal structure of GS441524 monophosphate, NSP12 8 and NSP7 of SARS-CoV-2 virus has been reported. By analyzing the crystal structure of NSP7,8 and 12, we found that the main interaction of the metabolite Remdesivir (GS441524 monophosphate) is with NSP12. This binding site overlap was seen using two available NSP7,8 and 12 crystal structures. Naringenin as a potential inhibitor of the SARS-CoV-2 RNA Polymerase was investigated. In an *in silico* analysis study, the compound have illustrated a similar pharmacophore to Nelfinavir. AutoDock software version 4.2 was used to investigate molecular interaction. As indicated by AutoDock results, the control drug molecule RDV was shown to have docking scores of  $-3.45$  kcal/mol and  $-4.32$

kcal/mol against NSP12 and NSP3, respectively. Also, naringenin had  $\Delta G$  values more than the  $\Delta G$  values RDV and GS-441,524; hence, naringenin was considered a potential inhibitor. Based on docking studies, El-Aziz et al. [34]. that showed several compounds on the 6M71 structure, respectively, RDV, gallic acid, quercetin, caffeine, ribavirin, resveratrol, naringenin, benzoic acid, oleuropein, and Ellagic acid have the highest binding energy to NSP12. Moreover, naringenin showed binding energy of  $-5.69$  (kcal/mol), indicating that docking with higher execution times achieves more accurate results. In the study of El-Aziz et al., naringenin bound with the amino acids Arg553, Arg555, Ser686 and Thr556 [34]. However, our results exhibited that naringenin binds with (C-chain) amino acids Gln31 and Ser60 of NSP12 and with binding energy of 7.54 and (C-chain) with amino acids Leu126, Ala129, Ser128 and Asn40 in NSP3. The naringenin connection to NSP3 was more robust than the NSP12 and needs to be tested with different software. Also, in the El-Aziz study, RDV reported  $-8.51$  (Kcal/ mol) binding energy with

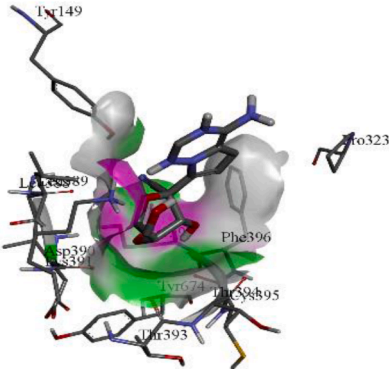
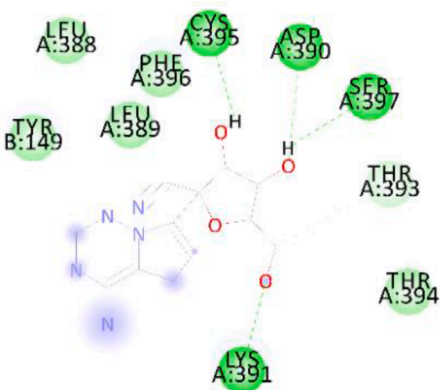
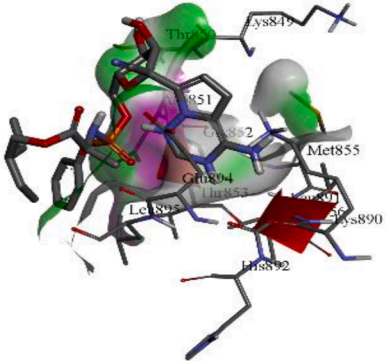
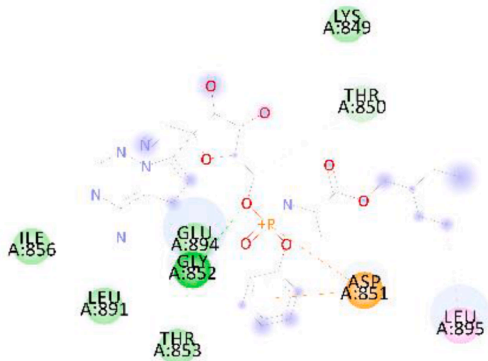
**Table 2**

Nonbonding interactions of naringenin with SARS-CoV-2 macrodomain RNA polymerase (NSP3) and SARS-CoV-2 RNA-dependent RNA polymerase (NSP12) (pose predicted by AutoDock and visualized by Discovery studio visualizer).

Protein	Ligand	H bond Interaction	2D Interaction
NSP3	Naringenin		
GS-441524			
Remdesivir			
NSP12	Naringenin		

(continued on next page)

Table 2 (continued)

Protein	Ligand	H bond Interaction	2D Interaction
	GS-441524		
	Remdesivir		

amino acids Asn691, Cys622 and Lys621, Tyr619, Thr680 and Thr687 residues [34]. Although, our results displayed that Gly852 forms a hydrogen bond, and with a binding energy of  $-3.45$  (Kcal / mol). RDV (Gs-5734) a prodrug of the adenosine monophosphate analog Gs-441, 524, was initially developed due to its strong antiviral activity in vitro to fight the Ebola virus [35]. Biochemical studies have shown that RDV, similar to natural nucleoside, combines in RNA formation in the presence of virus RNA-dependent RNA polymerase (RdR), but this does not occur for human DNA or RNA-dependent RNA polymerases [36–39]. The present study also showed that naringenin could inhibit NSP12 and significantly inhibit NSP3. The amino acids Lys545, Arg555 and Asn91 of COVID-19 RNA polymerase are predicted to be involved in the interaction [40].

Zhang et al., demonstrated the first RemTp (RDV active form) interactions with a mutated NSP12 that registered with the 6NUR PDB code [41]. They determined the main position of RDV active form, communicating with the positive charges of the amino acid units Lys798, Lys621, Arg555, Arg553, Lys551, and Arg836, which was also edenosine triphosphate (ATP) portion. RDV blocked the main function of the NSP12, 8 and NSP7 polymerase complexes [41]. Also, since other articles have reported RemTp binding to Asp618, there are more interactions that require investigation in further study [42]. When Thazolone derivatives VXR (VXR) bound to NSP12 with the binding energy of  $-23.23$  kcal/mol. These hydrogen bonds engaged amino acids Gly591, Gly590 and Lys593. Furthermore, Val588, Leu589, Ser592, Phe593, Trp598, Met601, Met756, Leu758, Phe812, Cys813, Ile864 and Asp865 residues made hydrophobic bonding.

In NSP7/NSP8/NSP12-VXR complexes with binding energy of 7–8 kcal/mol generated hydrogen bonds with Gly90, Thr591 and Lys593 residues. VXR also established hydrophobic bonding with amino acids Val588, Leu589, Ser592, Lys593, Phe5, Met601, Met756, Leu758, Phe812, Cys813, Ile869 and Asp865 [43]. These findings are robustly confirmed by similar form of ligand-protein interaction in presented

study. Our outcomes further proved the importance of the aforementioned residues in the targeting of the RdR.

### 3. Molecular dynamic (MD) simulation

Based on parameter simulation as described in (Table 3), we conclude that the structural dynamics and flexibility of NSP3 protein decreased in the presence of naringenin ligand. Furthermore, ligand-free NSP3 was more flexible, which could be related to the ligand coordination mode. Based on (Table 4) information, naringenin has strong interaction with NSP3 protein and, therefore, can be considered a potential medicine for COVID-19.

#### 3.1. Root mean-square deviation (RMSD)

Fig.3A depicts the changes in the RMSD in the simulation of NSP3, alone (Blue graph), and its complexes with naringenin (red graph), at 50 ns simulation time. Although oscillation and instability were observed at the beginning of the simulation time, the system reached a steady state after 30 ns, and the amount of RMSD fluctuations decreased. As shown in (Fig.3), the last 30 ns of MD simulation trajectories were used to calculate average RMSD that decreased for the NSP3 in complex with naringenin ( $5.55 \pm 1.58$  to  $3.45 \pm 0.56$  value) during simulation time. Here, ligand free NSP3 and NSP3-naringenin complexes RMSD values  $5.55 \pm 1.58$  nm and  $3.45 \pm 0.56$  nm, respectively, that showed stability, especially in the presence of ligand. In fact, in the first five ns of dynamic simulation, the NSP3 RMSD values increased to 10 nm and then stabilized between 0.5 to 1 nm, indicating that naringenin perfectly blocked NSP3. Elkarhat et al. (2020), Showed that STDs and VXRs also reduce RMSD levels [43]. The RMSD plot for NSP12 displayed that naringenin had negligible impact on the stability of NSP12. The average of the RMSD support that naringenin had not considerable impact to generate a stable complex (Fig.3B and Table3).

**Table 3**

The average and standard deviations of Rg, Area per residue, RMSD, RMSF, H-bond between protein-protein H-bond between protein-solvation (number) and NSP3 protein with naringenin.

Name	RMSD (nm)	Rg (nm)	RMSF (nm)	Area per residue (ASA) (nm)	H-bond between protein-protein (number)	H-bond between protein-solvation (number)
NSP3-Water	5.55±1.58	6.73±0.87	3.14±0.45	0.55±0.10	498±11	1109±25
NSP3-Naringenin	3.45±0.56	4.95±0.36	1.50±0.31	0.55±0.10	496±13	1105±35
NSP12-Water	0.23±0.01	3.58±0.03	0.129±0.064	0.62±1.44	800±20	1350±20
NSP12-Naringenin	0.24±0.021	3.59±0.01	0.118±0.058	0.62±1.44	799±14	1350±15

ave±SD

**Table 4**

The average values and standard deviations of temperature (K) of kinetic (EKCMT) and potential (EPTOT) and total (ETOT) energies (kJ/mol), Volume (nm<sup>3</sup>) and Density (kg/m<sup>3</sup>).

Name	EPTOT (KJ/mol)	EKCMT (kJ/mol)	ETOT (kJ/mol)	Temperature (K)	Volume (nm <sup>3</sup> )	Density (kg/m <sup>3</sup> )
Water	-1977032±1674.92	364359.8±1099.48	-1612672±1569.02	299.91±0.90	1486.43±2.04	1001.04±1.37
Naringenin	-1980084±35144.44	364487.4±1057.66	-1615597±35117.86	299.93±0.87	1486.61±7.11	1001.26±5.02

### 3.2. Root mean square fluctuation (RMSF)

Fig. 4 shows the rate of RMSF changes for each of the amino acid of the protease protein alone (Blue graph) and the NSP3 docked with the naringenin (red graph) throughout 50 nanoseconds. The most significant reduction in RMSF fluctuations occurred in naringenin-docked protein. The inhibitory effects of naringenin on the fluctuations of protease residues demonstrated that naringenin could inhibit amino acid residues of 150–170, 220–250 and 410–420, as well as 610 amino acid residues in the NSP3.

The RMSF values of NSP3 amino acid units in the presence of naringenin in NM were  $1.5 \pm 0.31$ , but when ligand-free NSP3 was simulated, the RMSF was  $3.14 \pm 0.45$  nm. NSP3 RMSF fluctuated between 4.4 and 2 nm, but in NSP3-naringenin complex fluctuated between 2.4 and 0.8 nm. C-chain flexibility, which includes amino acids of 343 to 514, had the most fluctuations (amino acids 410 to 430), indicating C-chain flexibility played an essential role in NSP3 flexibility. The A chain residues in NSP3 had the least flexibility and the lowest amplitude of RMSF fluctuations 1.2 to 2 nm. Against RMSD, the RMSF changes for NSP12 exhibited that the residues fluctuation relatively decreased, however the fluctuation changes was not remarkable. The RMSF results indicated that naringenin could bind to the active site of COVID-19 RNA polymerase. The RMSF values of NSP12 residues in NSP12-naringenin complex were decreased than ligand free NSP12.

### 3.3. The radius of gyration (Rg)

Fig. 5 describes the rate of radius of gyration (Rg) alterations of protease protein alone (Blue graph) and NSP3-naringenin complex (red graph) throughout 50 nanoseconds from the simulation time. (Fig. 5A), reveals an oscillation in the Rg rate during the simulation time. Limitation in the Rg rate demonstrated that distribution of the protein atom around its axis is diminished, accordingly the protein is stabilized in the presence of ligand. However, the mean rotational radius for the duct proteins with naringenin decreases during the simulation time. The changes in the Rg NSP3 was  $6.73 \pm 0.87$  nm (ranging between 5 and 8 nm), and when the protein was accompanied by naringenin, this value decreased to  $4.95 \pm 0.36$  nm. (Fig. 5B), exhibit acceptable stability for NSP12-naringenin complex. The Rg value for ligand free NSP12 and NSP12-naringenin complex were close. The average of the Rg for NSP12-naringenin in Table 3 displays slight fluctuation along with simulation

time, suggesting proper folding of the protein.

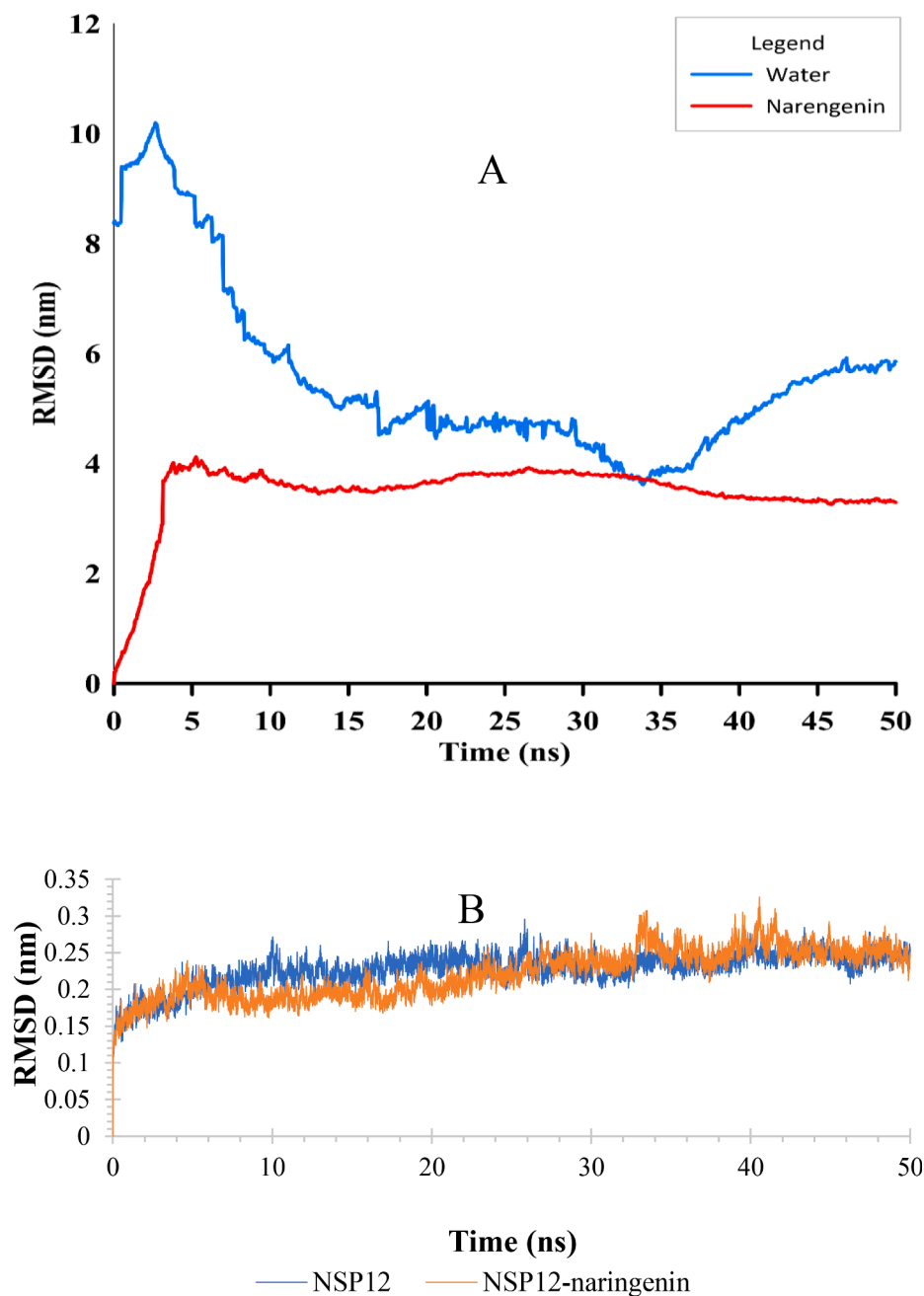
### 3.4. Hydrogen bonds (H-bound)

Fig. 6 demonstrates the rate of alterations in hydrogen bonds of protease protein (Blue graph), and NSP3-naringenin (red graph), over 50 nanoseconds of the simulation time. Accordingly, (Fig. 6) shows that during the simulation time, a slight decrease in hydrogen bonds was induced in the docked protein to naringenin compared ( $496 \pm 13$ ) to the protein alone ( $498 \pm 10$ ). The number of hydrogen bonds among intra-structure of NSP3, and inter-structure of NSP3-naringenin during simulation time equals  $498 \pm 11$  and  $1109 \pm 25$ , respectively. In NSP3-naringenin complex hydrogen bond values between intra-structure of NSP3 and protein-solvent gained  $496 \pm 13$ , and  $1105 \pm 35$  nm, respectively. These outcomes demonstrated that the number of hydrogen bonds within NSP3 protein and protein-solvent did not change much.

### 3.5. Secondary structure

Fig. 7 demonstrates the rate of alterations in the secondary structures of the free ligand NSP3 protein (Blue graph), and the NSP3-naringenin complexes (naringenin diagram), after 50 nanoseconds of the simulation time. Docked naringenin in NSP3 protein causes a augmentation in the  $\beta$ -Bridge structure ( $7.75 \pm 3.18$ ) and  $\beta$ -sheet to  $127.24 \pm 6.63$ . However, Coil, Turn and Bend, Helix structures were decreased. The augmentation in the  $\beta$ -Bridge,  $\beta$ -sheet structures percent and reduction in the Coil, Turn and Bend structures exhibited that protein robustly stabilized in the presence of ligand. All MD simulation outcomes proved that so naringenin made a stable and robust complex.

Phosphates functional group showed a higher interaction than pro-drug and other intermediate metabolites in the RMSF, RMSD and Rg analysis on the structure of RdR [44]. The study of Celik et al. [44], using a molecular dynamics approach has indicated that the antiviral drugs favipiravir, remdesivir, galidesivir, and ribavirin prevented virus replication by inhibiting virus RNA-dependent RNA polymerase. MD outcomes of this study also report strong and stabilized bonds among NSP3-naringenin.



**Fig. 3.** Changes in the Root mean square deviation (RMSD) during 50 nanoseconds simulation time. A. the blue curve correspond to the RMSD of protein alone (Water) and the red curve correspond to the RMSD of protein-ligands (naringenin). B. The blue curve display ligand free NSP12 RMSD and the orange curve present the NSP12-naringenin complex RMSD.

#### 4. Physiochemical, pharmacokinetic, and ADMET properties of naringenin

Pharmacokinetic properties and prediction of ADMET properties of naringenin and RDV were calculated using PKCSM web tool. The results of toxicity prediction and physicochemical properties are shown in (Table 5). The results showed that the two compounds had no significant potential cytotoxicity effect. Naringenin had less brain damage than RDV and had high digestive absorption. Naringenin has slightly more solubility than RDV, but this difference may not be significant. The AMES toxicity for naringenin was positive, thus this compound had potential mutagenicity effect. However, based on the some clinical study, Naringenin has not any mutagenic, teratogenic and carcinogenic effect with daily ingestion of 150 to 900 mg doses. Thus, Naringenin can

used for clinical study with daily dose of 900 mg [45].

The penetration, distribution of RDV are higher than that of naringenin. Both compounds have CYP induction and P-gp compatibility. The PSA of the RDV drug is greater than 140, which means has strong polarity and therefore is not easily absorbed by the body. But PSA is 86.99 for naringenin, so it is easily absorbed. Two compounds (naringenin and RDV) have good membrane thermal absorption or permeability, because log P was less than 5. logBB demonstrated that compounds would not cross the blood-brain barrier. Cytochrome P450 (CYP) is a vital enzyme system for drug metabolism in the liver. In contrast to naringenin, RDV is a substrate for CYP3A4. naringenin was a CYP3A4 inhibitor, while RDV did not. Thus, naringenin is metabolized in the liver. The hERG (the human Ether-à-go-go-Related Gene) is potassium ion channel, and essential for normal electrical activity in the

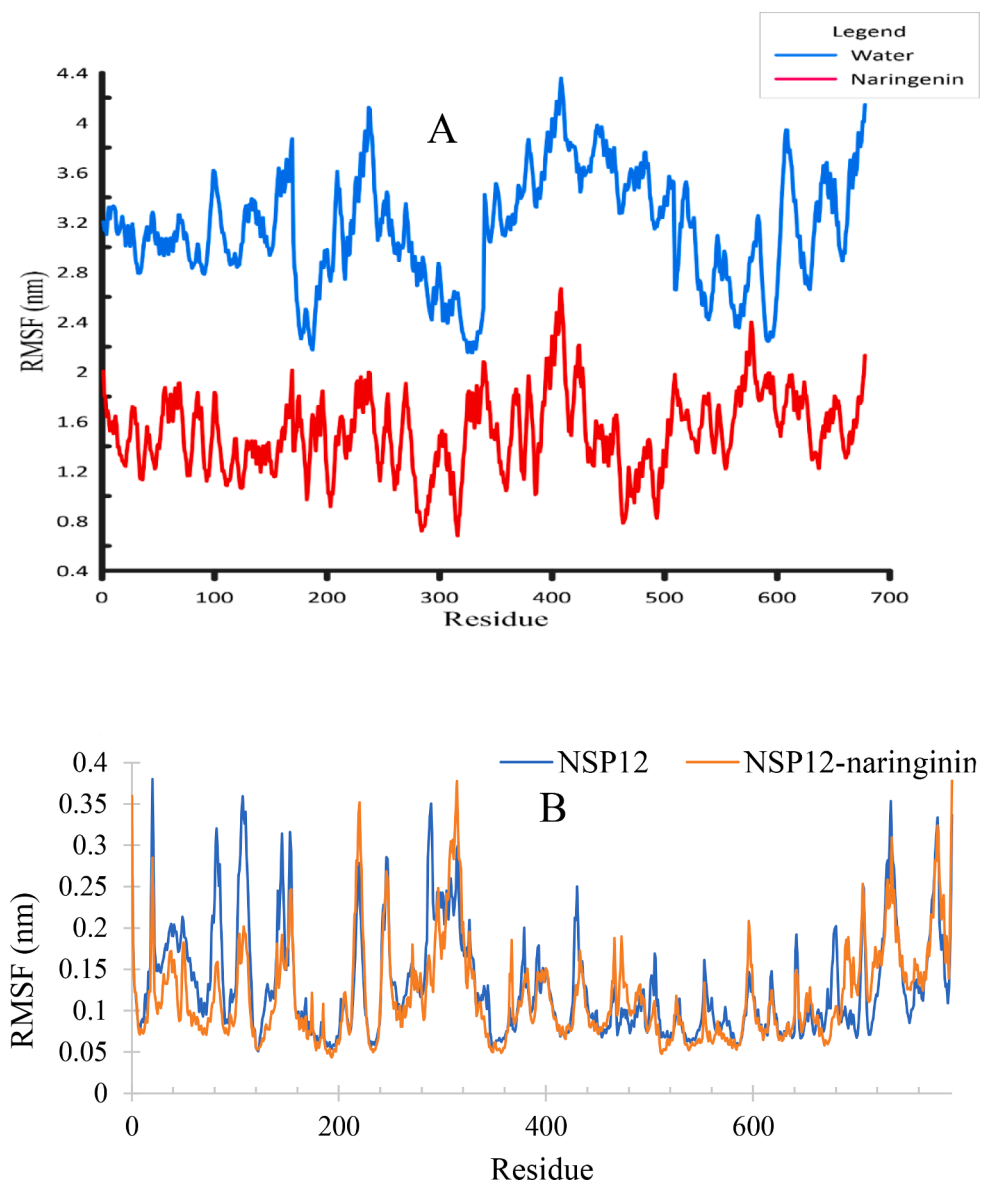


**Fig. 4.** Changes in Root mean square fluctuation (RMSF) during 50 nanoseconds simulation time. A. the blue curve correspond to the RMSF of protein alone (Water) and the red curve correspond to the RMSF of protein-ligands (naringenin). B. RMSF analyses of naringenin-NSP12 complex. The blue curve display ligand free NSP12 RMSF and the orange curve present the NSP12-naringenin complex RMSF.

heart. These two compounds did not inhibit the hERG 1 channel and inhibited hERG 2, however, on the clinical trial studies, did not show the inhibitory cardiac effects with daily ingestion of 150 to 900 mg doses Naringenin [31].

Some reports show flavonoids have several biological functions against some viruses [46]. Some tests have been done to evaluate the antiviral function of the flavanone naringenin versus some types of viruses, including HCV, Chikungunya virus (CHIKV), Dengue virus (DENV), and Zika virus (ZIKV) [47]. Also, it was shown that using naringenin led to the silencing of the apoB mRNA in the infected cells and reduced 70% release of both apoB100 and HCV [48]. Another study showed that naringenin administration could inhibit ZIKV infection in human A549 cells in a concentration-dependent manner. As the primary human monocyte-derived dendritic cells were cured after infection, the antiviral function of naringenin was also uncovered. Consequently, this result indicates that naringenin can reduce viral reproduction or assembly of viral elements. Also, an interaction among the protease domain of the NS2B-NS3 protein of ZIKV and naringenin can describe the anti-ZIKV function of this compound [46].

Five important pharmacokinetic parameters including absorption, distribution, metabolism, excretion, and toxicity (ADMET) are important factors in converting a designed compound into a suitable drug candidate [30,49]. Naringenin could only act as P-gp substrates, which reduces its clinical effect. Drug concentration at the site of drug uptake is affected by many factors, including lipid solubility, plasma concentration, and the ability to bind to plasma and transport proteins [33,50].

There is a relationship between chemical structures and physicochemical properties. Therefore, chemical descriptors can be used to calculate pharmacokinetic properties. Polar Surface Area (PSA) is a superficial descriptor used to measure drug permeability. It is defined as part of the surface area created by nitrogen, oxygen, and the hydrogen atoms attached to them [51]. Brain-blood partition coefficient (LogBB) shows the rate at which molecules cross the blood-brain barrier. In addition, evaluation of the risk parameters of toxicity and medicinal properties of the designed compounds showed that naringenin had no risk tumorigenesis, inflammatory effects and toxic effects (Table 6). In general, it can be concluded that perhaps naringenin is in an acceptable range in terms of toxicity and medicinal properties, considering this



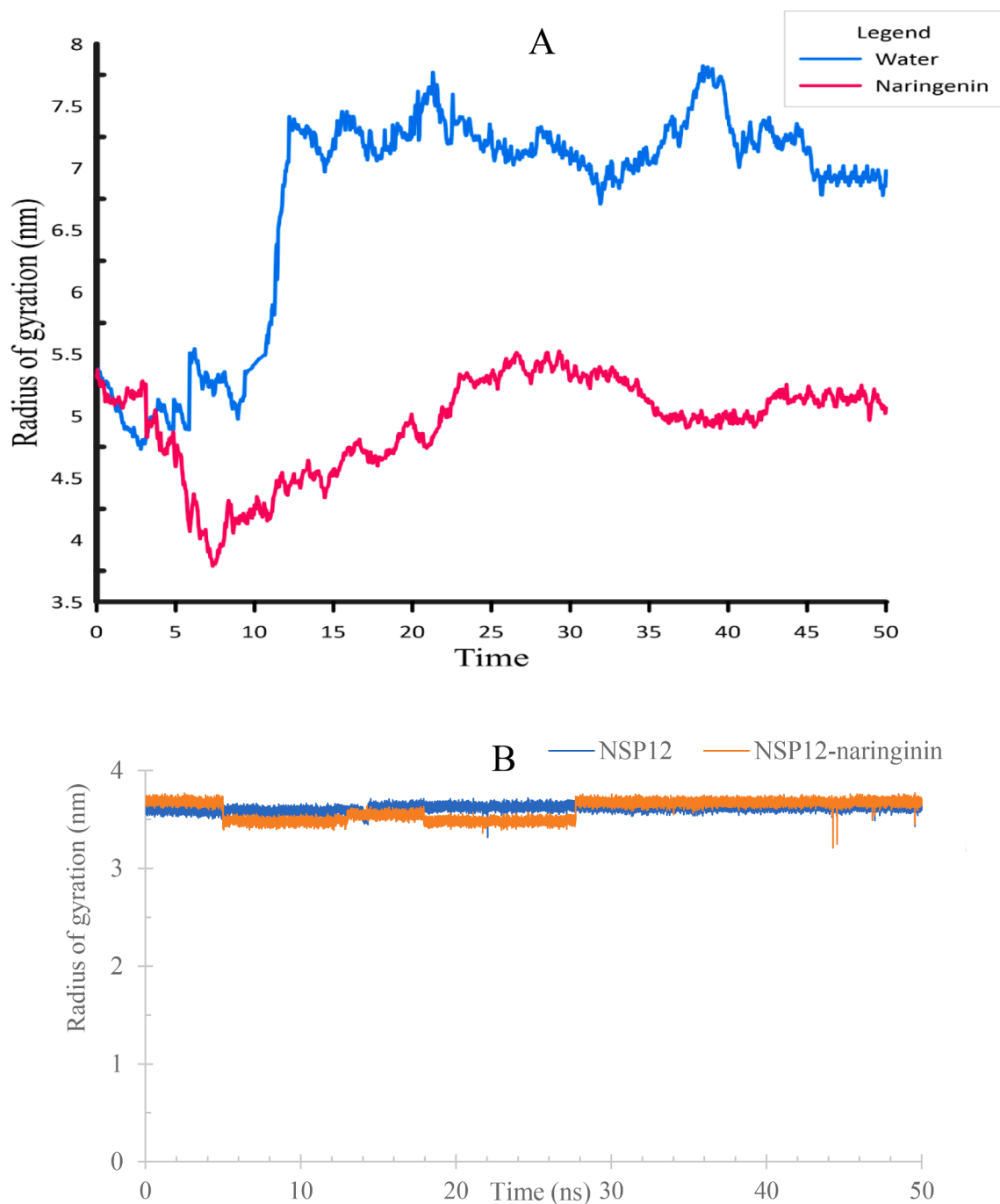


**Fig. 5.** Changes in the Radius of gyration (Rg) during 50 nanoseconds simulation time. (A) The Blue curve corresponds to Rg of protein (NSP3) alone (Water) and the red curve correspond to the Rg of protein-naringenin). (B) The blue curve display ligand free NSP1 Rg and the orange curve present the NSP12-naringenin complex Rg.

compound a valid drug. ADMET results displayed that, because of the low bioavailability and quick metabolism, accordingly deletion of almost all flavonoids such as naringenin. Therefore maybe, there is less possibility of adverse effects reported by using them [52]. Also, the outcomes showed no adverse effects in a clinical study across the healthy overweight subjects that evaluated the efficacy and safety of polyphenolic citrus dry extract such as naringenin [53]. Nevertheless, since there is not enough evidence on the safety and toxicity of naringenin, utilizing this flavanone in clinical trials on SARS-CoV-2 must be planned cautiously [54].

## 5. Materials and methods

Remdesivir (RDV) was introduced as an antiviral drug and an inhibitor of RNA-dependent RNA polymerase. In this study, Molecular Docking was used to determine the behavior of RDV drug and its metabolic derivatives (GS-441,524) with two structures, including SARS-CoV-2 RNA dependent RNA polymerase (NSP12) and SARS-CoV-2 macrodomain RNA polymerase (NSP3). Naringenin was also chosen for this study due to its profound bioactive impact, including antioxidant, free radical scavenger, anti-inflammatory, carbohydrate metabolism promoter, and immune system modulator. The molecular dynamics behavior of NSP3 in the presence of naringenin compound was

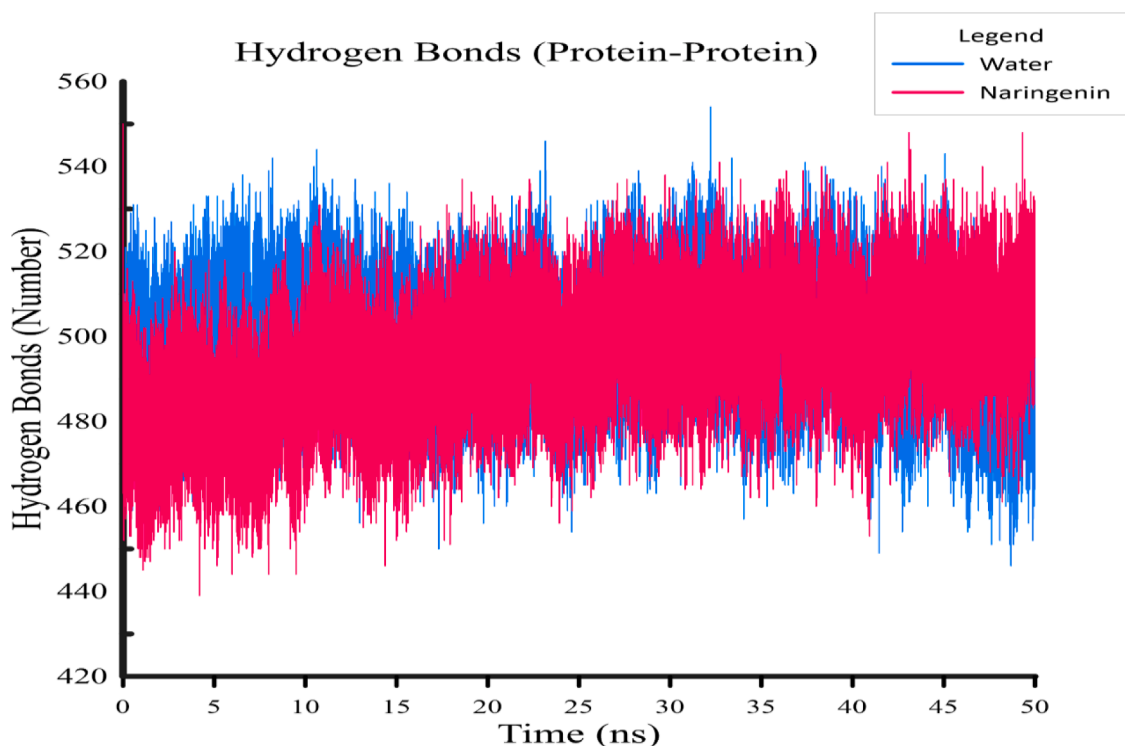


**Fig. 6.** Changes in the number of hydrogen bonds during 50 nanoseconds simulation time. Naringenin and NSP-3. The Blue curve correspond to the number of hydrogen bonds of protein alone (Water) and the red curve correspond to the number of hydrogen bonds of a protein–ligands complex.

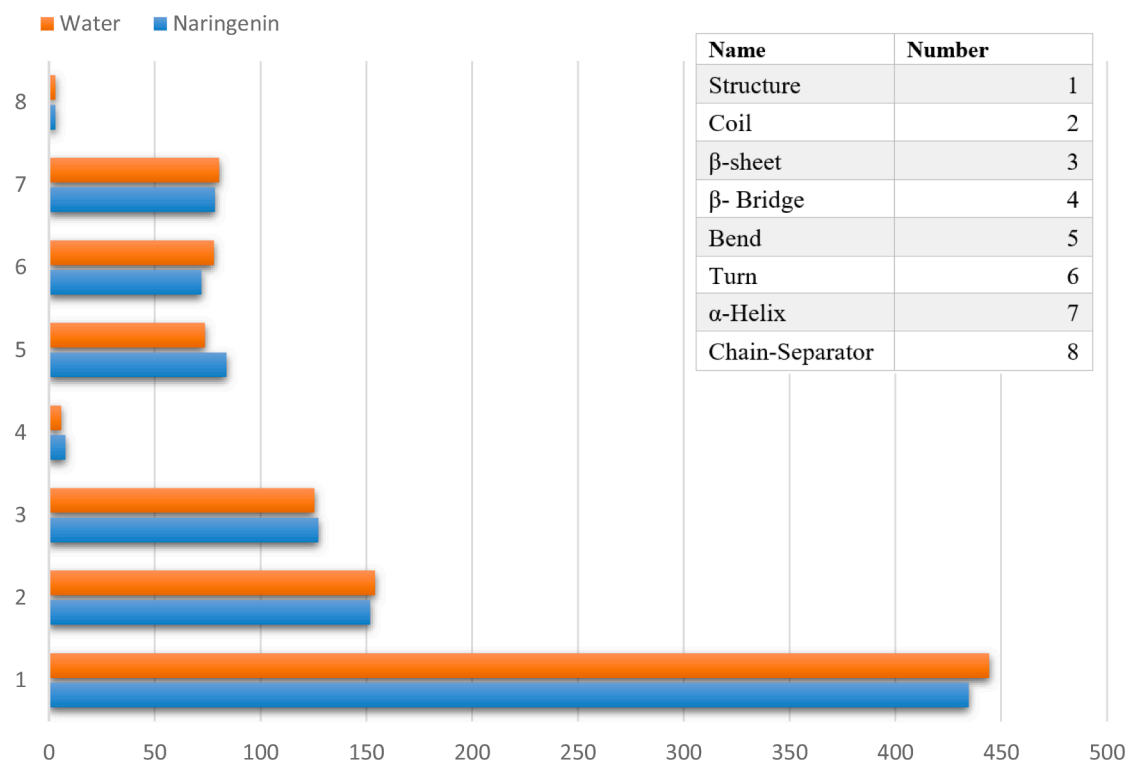


**Fig. 7.** Changes in the secondary structures during 50 nanoseconds simulation time. The orange, and blue rows display water and naringenin, respectively.

investigated with GROMACS 2018.1 software (Table 6).

### 5.1. Protein retrieval and preparation

The protein data bank (PDB) file of RNA-dependent RNA polymerase

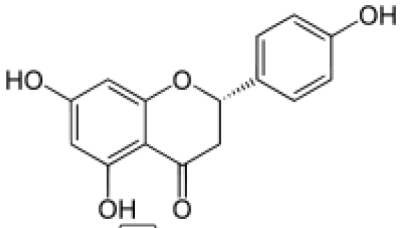
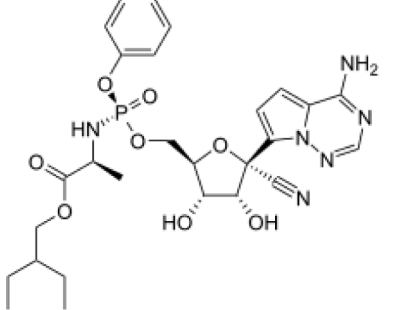
(NSP12) (PDB ID: 6M71) and SARS-CoV-2 macrodomain RNA polymerase (NSP3) (PDB ID: 6WOJ) were obtained from the protein data bank server ([www.rcsb.org](http://www.rcsb.org)). Subsequently, the hydrogen atoms were added in pH=7 and water molecules were omitted, using Discovery Studio software 2.5 (DS, Accelrys Inc, San Diego) [55,56]. Energy

**Table 5**  
Predicted ADMET properties of naringenin and Remdesivir.

Properties	Naringenin	Remdesivir
Polar Surface Area (PSA)	86.99	213.36
LogP	1.84	1.53
Synthetic accessibility	3.01	6.33
Water solubility (log mol/L)	-3.278	-3.089
Caco2 per. (log Papp in 10 <sup>-6</sup> cm/s)	1.166	0.577
Intestinal ab (human) (% Absorbed)	90.508	64.198
Skin Permeability (log Kp)	-3.225	-2.735
P-gp substrate	Yes	Yes
P-gp I inhibitor	No	Yes
P-gp II inhibitor	No	Yes
VDss (human) (log L/kg)	-0.029	0.984
Fraction unbound (human) (Fu)	0.18	0.088
BBB permeability (log BB)	-0.969	-2.005
CNS permeability (log PS)	-2.236	-4.115
(log ml/min/kg)	No	No
CYP3A4 substrate	No	Yes
CYP1A2 inhibitor	Yes	No
CYP2C19 inhibitor	No	No
CYP2C9 inhibitor	No	No
CYP2D6 inhibitor	No	No
CYP3A4 inhibitor	Yes	No
Total Clearance (log ml/min/kg)	0.068	0.184
Renal OCT2 substrate	No	No
AMES toxicity	Yes	No
MTD @ (log mg/kg/day)	0.402	-0.164
hERG 1 inhibitor	No	No
hERG 2 inhibitor	Yes	Yes
ORT* (mol/kg)	2.189	2.027
ORCT# (log mg/kg_bw/day)	1.994	2.677
HEP\$	No	Yes
SS <sup>+</sup>	No	No
TPT+ (log ug/L)	0.69	0.285
Minnow toxicity (log mM)	0.616	1.112
Molecular Weight	272.25	602.58

Synthetic accessibility range (0-10) = very easy to very difficult to synthesize; \*P-gp- P-glycoprotein; @MTD-Max. tolerated dose (human); \*ORT-Oral Rat Acute Toxicity (LD50); #ORCT- Oral Rat Chronic Toxicity (LOAEL); HEP \$-Hepatotoxicity; ^SS-Skin Sensitization; +TPT-Pyrimidism toxicity.

**Table 6**  
Ingredients of naringenin compound used for *in silico* screening against proteins of SARS-CoV-2 RNA polymerase

Sr. No	Ligand	Molecular Formula	Molar mass (g/mol)	PubChem CID	Structure
1	Naringenin	C15H12O5	272.257	932	
2	Remdesivir	C27H35N6O8P	602.58	121304016	

minimization was performed till energy gradient fell in 0.1 calÅ<sup>-1</sup> by Discovery Studio and Swiss-PdbViewer (aka DeepView).

### 5.2. Positive control and preparation of ligand structure

Four RDV forms, were selected as positive controls for the execution of blind docking. Their structure was also acquired in PDB format from the <https://go.drugbank.com/> website. The three-dimensional structure (PDB) of all three ligands (RDV, naringenin and GS-441,524) was downloaded from the PubChem server (<https://pubchem.ncbi.nlm.nih.gov/>). Ligands were finally minimized with the Gasteiger charges by Chimera 1.13.1 software [57].

### 5.3. Molecular docking

The molecular docking study was performed using AutoDock software version 4.2 [58]. The above-mentioned ligands were docked on the NSP12 and NSP3 COVID-19 as receptors to determine the ligand's most stable free energy state. In the current study, a grid box with dimensions of 60 × 120 × 90 (x × y × z) with default AutoDock grid spacing of 0.375 Å was created to dock ligands in receptor. The Genetic Algorithm and Lamarckian GA parameters with maximum number of generations simulated during each GA or LGA run=27,000 and maximum number of energy evaluations performed during each GA, LGA, or LS run=25,000, 00. The AutoDock4 version Linux was used to generate the results file (dlg). The obtained data from the dlg file was analyzed [58]. The estimated inhibition constant (K<sub>ex</sub>) is Computed by the equation [59].

$$K_{ex} = \exp[(\Delta G_{ex} \times 1000 / RT)]$$

$\Delta G_{ex}$  is a semiempirical free energy approximation (derived from molecular mechanics and experimental parameters), R is 1.98719 cal.K<sup>-1</sup>.mol<sup>-1</sup>, and T is 298.15 K [59]. Discovery Studio Visualizer software was used to specify the number of hydrophobic and hydrogen bonds between the receptors with each ligand. Furthermore, the type and number of existing amino acids in the binding site were determined [60].

### 5.4. Molecular dynamics simulations

Molecular dynamics is a computer simulation of the atoms' and molecules' physical movements over a period of time. During this

period, the motion of atoms would be investigated. In most molecular dynamics simulations, the system's initial conditions are far from equilibrium. Therefore, the first simulation step in molecular dynamics must be done at equilibrium time for the system to reach the equilibrium state. While equilibrium is gained, the thermodynamic and structural properties of the compound are controlled until it finally reaches stability level. In this research, molecular dynamics simulation of the studied complex was conducted, using GROMACS 2018.1 software at constant pressure and temperature (NPT) [61]. All the proteins topologies were generated from the G43a1 force field. The ITP and gro ligand files were created from the PRODRG database [62]. All complexes were solvated with the extended simple point charge (SPC216) water model in a cubic box of 1.0 nm distance from the protein to the surface under periodic boundary conditions box. Sodium and chloride ions were injected to neutralize each system, then the steepest descent integrator technique was used to minimize energy. Following that, the constant temperature of 300 K for 100 ps and 1 bar pressure were applied to equilibrate the systems. For the simulations, the isotropic Monte Carlo (MC) barostat and the Nose Hoover thermostat were used to maintain the pressure at 1 atm. Lennard-Jones potential and Particle Mesh Ewald (PME) calculations were performed to handle Van der Waals and electrostatic interactions, respectively. Finally, 50 Nanoseconds (ns) MD simulation run with 1fs time step were done on each complex. The 2D plots representing the intrinsic dynamical stabilities of the complex such as RMSD, RMSF, Rg, and hydrogen bond interactions between the protein and compound were generated [63].

### 5.5. Physicochemical, pharmacokinetic, and ADMET properties of naringenin

The crucial criteria consisting of physicochemical qualities, non-toxicity, and pharmacological effectiveness computations were performed to select a molecule as a therapeutic candidate. Therefore, in the present study, physicochemical properties of RDV and naringenin were predicted, including water solubility, polarization rate (TPSA), diffusion (logD) and metabolism. The inhibitory effect of compounds on phase I metabolism enzymes, including CYP1A2, CYP2C19, CYP2C9, CYP3A4 and CYP2D6 were investigated by the SwissADME server ([www.swissadme.ch](http://www.swissadme.ch)) [64]. This server provides the possibility of predicting physicochemical properties and cytotoxicity by receiving information on chemical molecules in the form of mol or SMILE file. In addition, the mutagenic potential of the studied compounds was predicted by ToxTree.2.6 software [65].

## 6. Conclusion

The affinity of naringenin bonds is higher compared with remdesivir. Naringenin with connection to NSP3 can stabilize it and could inhibit it. Therefore, we suggested that naringenin may represent potential treatment options. However, further research is necessary to investigate the potential uses of medicinal plants containing these compounds. The approach of developing a drug through naringenin with its NSP binding sites is a promising choice to treat modified SARS-CoV-2 viruses. But further "in vitro" and "in vivo" experiments should be performed to reveal these interactions. Since naringenin is an organic compound and metabolized in the human body, an adverse effect has not been reported, so it suggested that a synergistic effect of naringenin with RDV must be studied in a clinical trial study. Due to the antiviral and anti-inflammatory effects of naringenin and the favorable interaction of this flavonoid compound with the SARS-CoV-2 RNA polymerase, it can provide a way to find an effective treatment for COVID-19 infection.

### Credit author statement

Ghoshouni H, Koochaki P, Esmaili-Dehkordi M, Alebrahim E, Chichagi F, Jafari A, Heidari-Soureshjani E, Investigation, Software, Writing

and prepared the initial draft; Alebrahim-Dehkordi E, study design, Data curation and Formal analysis, Idea and the initiator of the figures, Project administration, writing-final draft and editing; Hanaie S, Writing-review and editing; Rezaei N, Supervision the project, Validation and critically appraised the manuscript. All authors contributed to the article and approved the submitted version.

### Funding

This research did not receive any specific grant from funding agencies in the public, commercial, or not-for-profit sectors.

### Declaration of Competing Interest

The authors declare that there is no conflict of interests.

### Data availability

Data will be made available on request.

### Acknowledgments

We would like to thank SaNa Zist Pardaz company for their parts in the development and support of the softwares for Docking and Simulation. also, The authors would like to thank Dr Azhar Salari-Jazi, for the invaluable assistance and providing computation consulting.

### References

- [1] E. Alebrahim-Dehkordi, A. Reyhanian, A. Hasanpour-Dehkordi, Clinical Manifestation and the Risk of Exposure to SARS-CoV-2 (COVID-19), *Int. J. Prev. Med* 7 (2020) 11–86, <https://doi.org/10.4103/2008-7802.289255>.
- [2] Y. Yang, Q. Lu, M. Liu, Y. Wang, A. Zhang, N. Jalali, N.E. Dean, I. Longini, M. E. Halloran, B. Xu, X.A. Zhang, L.P. Wang, W. Liu, L.Q. Fang, Epidemiological and clinical features of the 2019 novel coronavirus outbreak in China, *medRxiv* (2020), <https://doi.org/10.1101/2020.02.10.20021675>.
- [3] L. Fang, Receptor recognition mechanisms of coronaviruses: a decade of structural studies, *J. Virol.* 89 (2015) 1954–1964, <https://doi.org/10.1128/JVI.02615-14>. Epub 2014 Nov 26.
- [4] W. Li, S.K. Wong, F. Li, J.H. Kuhn, I.C. Huang, H. Choe, M. Farzan, Animal origins of the severe acute respiratory syndrome coronavirus: insight from ACE2-S-protein interactions, *J. Virol.* 80 (2006) 4211–4219, <https://doi.org/10.1128/JVI.80.9.4211-4219.2006>.
- [5] L. Du, Y. He, Y. Zhou, S. Liu, B.J. Zheng, S. Jiang, The spike protein of SARS-CoV a target for vaccine and therapeutic development, *Nat. Rev. Microbiol.* 7 (2009) 226–236, <https://doi.org/10.1038/nrmicro2090>.
- [6] L. Du, Y. Yang, Y. Zhou, L. Lu, F. Li, S. Jiang, MERS-CoV spike protein: a key target for antivirals, *Expert Opin. Ther. Targets* 21 (2017) 131–143, <https://doi.org/10.1080/14728222.2017.1271415>.
- [7] A.J. Rodríguez-Morales, K. MacGregor, S. Kanagarajah, D. Patel, P. Schlagenhauf, Going global-Travel and the 2019 novel coronavirus, *Travel Med Infect Dis* 33 (2020), 101578, <https://doi.org/10.1016/j.tmaid.2020.101578>.
- [8] L. Dong, S. Hu, J. Gao, Discovering drugs to treat coronavirus disease 2019 (COVID-19), *Drug Discov Ther* 14 (2020) 58–60, <https://doi.org/10.5582/ddt.2020.01012>.
- [9] A.C. Kalil, Treating COVID-19-Off-Label Drug Use, Compassionate Use, and Randomized Clinical Trials During Pandemics, *JAMA* 19 (2020) 1897–1898, <https://doi.org/10.1001/jama.2020.4742>.
- [10] G. Li, E. De Clercq, Therapeutic options for the 2019 novel coronavirus (2019-nCoV), *Nat Rev Drug Discov* 19 (2020) 149–150, <https://doi.org/10.1038/d41573-020-00016-0>.
- [11] J.M. Sanders, M.L. Monogue, T.Z. Jodlowski, J.B. Cutrell, Pharmacologic Treatments for Coronavirus Disease 2019 (COVID-19): a Review, *JAMA* 12 (2020) 1824–1836, <https://doi.org/10.1001/jama.2020.6019>.
- [12] J.S. Morse, T. Lalonde, S. Xu, W.R. Liu, Learning from the Past: possible Urgent Prevention and Treatment Options for Severe Acute Respiratory Infections Caused by 2019-nCoV, *ChemBioChem* 21 (2020) 730–738, <https://doi.org/10.1002/cbic.202000047>.
- [13] H. Lu H, Drug treatment options for the 2019-new coronavirus (2019-nCoV), *Biosci Trends* 14 (2020) 69–71, <https://doi.org/10.5582/bst.2020.01020>.
- [14] M. Romano, A. Ruggiero, F. Squeglia, G. Maga, R. Berisio, A Structural View of SARS-CoV-2 RNA Replication Machinery: RNA Synthesis, Proofreading and Final Capping, *Cells* 9 (2020) 1267, <https://doi.org/10.3390/cells9051267>.
- [15] A. Wu, Y. Peng, B. Huang, X. Ding, X. Wang, P. Niu, J. Meng, Z. Zhu, Z. Zhang, J. Wang, J. Sheng, L. Quan, Z. Xia, W. Tan, G. Cheng, T. Jiang, Genome Composition and Divergence of the Novel Coronavirus (2019-nCoV) Originating in

- China, Cell Host Microbe 27 (2020) 325–328, <https://doi.org/10.1016/j.chom.2020.02.001>.
- [16] D.G. Ahn, J.K. Choi, D.R. Taylor, J.W. Oh, Biochemical characterization of a recombinant SARS coronavirus nsp12 RNA-dependent RNA polymerase capable of copying viral RNA templates, Arch. Virol. 157 (2012) 2095–2104, <https://doi.org/10.1007/s00705-012-1404-x>.
- [17] J.F.W. Chan, S.K. Lau, K.K. To, V.C. Cheng, P.C. Woo, K.Y. Yuen, Middle East respiratory syndrome coronavirus: another zoonotic betacoronavirus causing SARS-like disease, Clin. Microbiol. Rev. 28 (2015) 465–522, <https://doi.org/10.1128/CMR.00102-14>.
- [18] S. Perlman, J. Netland, Coronaviruses post-SARS: update on replication and pathogenesis, Nat. Rev. Microbiol. 7 (2009) 439–450, <https://doi.org/10.1038/nrmicro2147>.
- [19] A.E. Gorbalenya, S.C. Baker, R.S. Baric, R.J. de Groot, C. Drosten, A.A. Gulyaeva, B.L. Haagmans, C. Lauber, A.M. Leontovich, B.W. Neuman, D. Penzar, S. Perlman, L.L.M. Poon, D.V. Samborskiy, I.A. Sidorov, I. Sola, J. Ziebuhr, The species Severe acute respiratory syndrome-related coronavirus: classifying 2019-nCoV and naming it SARS-CoV-2, Nat. Microbiol. 5 (2020) 536–544, <https://doi.org/10.1038/s41564-020-0695-z>.
- [20] R. Arya, S. Kumari, B. Pandey, H. Mistry, S.C. Bihani, A. Das, V. Prashar, G. D. Gupta, L. Panicker, M. Kumar, Structural insights into SARS-CoV-2 proteins, J. Mol. Biol. 433 (2021), 166725, <https://doi.org/10.1016/j.jmb.2020.11.024>.
- [21] C.C. Posthuma, A.J. Te Velthuis, E.J. Snijder, Nidovirus RNA polymerases: complex enzymes handling exceptional RNA genomes, Virus Res. 234 (2017) 58–73, <https://doi.org/10.1016/j.virusres.2017.01.023>.
- [22] Z. Ruan, C. Liu, Y. Guo, Z. He, X. Huang, X. Jia, T. Yang, Potential Inhibitors Targeting RNA-Dependent RNA Polymerase Activity (NSP12) of SARS-CoV-2, Preprints (2020), 2020030024, <https://doi.org/10.20944/preprints202003.0024.v1>.
- [23] N.R. Sexton, E.C. Smith, H. Blanc, M. Vignuzzi, O.B. Peersen, M.R. Denison, Homology-Based Identification of a Mutation in the Coronavirus RNA-Dependent RNA Polymerase That Confers Resistance to Multiple Mutagens, J. Virol. 90 (2016) 7415–7428, <https://doi.org/10.1128/JVI.00080-16>.
- [24] A.J.W. te Velthuis, S.H.E. van den Worm, E.J. Snijder, The SARS-coronavirus nsp7 +nsp8 complex is a unique multimeric RNA polymerase capable of both de novo initiation and primer extension, Nucleic. Acids. Res. 40 (2016) 1737–1747, <https://doi.org/10.1093/nar/gkr893>.
- [25] L. Subissi, C.C. Posthuma, A. Collet, J.C. Zevenhoven-Dobbe, A.E. Gorbalenya, E. Decroly, E.J. Snijder, B. Canard, I. Imbert, One severe acute respiratory syndrome coronavirus protein complex integrates processive RNA polymerase and exonuclease activities, Proc. Natl. Acad. Sci. U.S.A. 37 (2014) E3900–E3909, <https://doi.org/10.1073/pnas.1323705111>.
- [26] Y. Zhai, F. Sun, X. Li, H. Pang, X. Xu, M. Bartlam, Z. Rao, Insights into SARS-CoV transcription and replication from the structure of the nsp7-nsp8 hexadecamer, Nat. Struct. Mol. Biol. 12 (2005) 980–986, <https://doi.org/10.1038/nsmb999>.
- [27] E. Alebrahim-Dehkordi, M. Rafieian-Kopaei, M. Bahmani, S. Abbasi, Antioxidant activity, total phenolic and flavonoid content, and antibacterial effects of Stachys lavandulifolia Vahl. flowering shoots gathered from Isfahan, J. Chem. Pharm. Sci 9 (2016) 3403–3408, <https://doi.org/10.1089/jmf.2013.0057>.
- [28] M. Wink, Modes of action of herbal medicines and plant secondary metabolites, Medicines (Basel) 2 (2015) 251–286, <https://doi.org/10.3390/medicines2030251>.
- [29] S. Kumar, A.K. Pandey, Chemistry and biological activities of flavonoids: an overview, Sci. World J (2013), <https://doi.org/10.1155/2013/162750>, 162750–162750.
- [30] M. Zobeiri, T. Belwal, F. Parvizi, R. Naseri, M.H. Farzaei, S.F. Nabavi, et al., Naringenin and its nano-formulations for fatty liver: cellular modes of action and clinical perspective, Curr. Pharm. Biotechnol. 19 (3) (2018) 196–205.
- [31] B. Salehi, P.V.T. Fokou, M. Sharifi-Rad, P. Zucca, R. Pezzani, N. Martins, et al., The therapeutic potential of naringenin: a review of clinical trials, Pharmaceuticals 12 (1) (2019) 11.
- [32] A. Frediansyah, F. Nainu, K. Dhama, M. Mudatsir, H. Harapan, Remdesivir and its antiviral activity against COVID-19: a systematic review, Clin Epidemiol Glob Health 9 (2021) 123–127, <https://doi.org/10.1016/j.cegh.2020.07.011>.
- [33] P.R. Nagar, N.D. Gajjar, T.M. Dhameliya, In search of SARS CoV-2 replication inhibitors: virtual screening, molecular dynamics simulations and ADMET analysis, J. Mol. Struct. 15 (2021), 131190, <https://doi.org/10.1016/j.molstruc.2021.131190>.
- [34] N.M. Abd El-Aziz, O.M. Eldin Awad, M.G. Shehata, S.A. El-Sohaimy, inhibition of the SARS-CoV-2 RNA-Dependent RNA polymerase by natural bioactive compounds: molecular docking analysis, Egypt. J. Chem. 64 (4) (2021) 1989–2001.
- [35] T.K. Warren, R. Jordan, M.K. Lo, A.S. Ray, R.L. Mackman, V. Soloveva, D. Siegel, M. Perron, R. Bannister, H.C. Hui, N. Larson, R. Strickley, J. Wells, K.S. Stuthman, S.A. Van Tongeren, N.L. Garza, G. Donnelly, A.C. Shurtleff, C.J. Retterer, D. Gharaibeh, R. Zamani, T. Kenny, B.P. Eaton, E. Grimes, L.S. Welch, L. Gomba, C. L. Wilhelmsen, D.K. Nichols, J.E. Nuss, E.R. Nagle, J.R. Kugelman, G. Palacios, E. Doerfler, S. Neville, E. Carra, M.O. Clarke, L. Zhang, W. Lew, B. Ross, Q. Wang, K. Chun, D. Babusis, Y. Park, K.M. Stray, I. Trancheva, J.Y. Feng, O. Barauskas, Y. Xu, P. Wong, M.R. Braun, M. Flint, L.K. McMullan, S.S. Chen, R. Fearnis, S. Swaminathan, D.L. Mayers, C.F. Spiropoulou, W.A. Lee, S.T. Nichol, T. Cihlar, S. Bavari, Therapeutic efficacy of the small molecule GS-5734 against Ebola virus in rhesus monkeys, Nature 531 (2016) 381–385, <https://doi.org/10.1038/nature17180>.
- [36] W. Yin, C. Mao, X. Luan, D.D. Shen, Q. Shen, H. Su, X. Wang, F. Zhou, W. Zhao, M. Gao, S. Chang, Y.C. Xie, G. Tian, H.W. Jiang, S.C. Tao, J. Shen, Y. Jiang, H. Jiang, Y. Xu, S. Zhang, Y. Zhang, H.E. Xu, Structural basis for inhibition of the RNA-dependent RNA polymerase from SARS-CoV-2 by remdesivir, Science 26 (2020) 1499–1504, <https://doi.org/10.1126/science.abc1560>.
- [37] C.J. Gordon, E.P. Tchesnokov, E. Woolner, J.K. Perry, J.Y. Feng, D.P. Porter, M. Götte, Remdesivir is a direct-acting antiviral that inhibits RNA-dependent RNA polymerase from severe acute respiratory syndrome coronavirus 2 with high potency, J. Biol. Chem. 15 (2020) 6785–6797, <https://doi.org/10.1074/jbc.RA120.013679>.
- [38] Q. Wang, J. Wu, H. Wang, Y. Gao, Q. Liu, A. Mu, W. Ji, L. Yan, Y. Zhu, C. Zhu, X. Fang, X. Yang, Y. Huang, H. Gao, F. Liu, J. Ge, Q. Sun, X. Yang, W. Xu, Z. Liu, H. Yang, Z. Lou, B. Jiang, L.W. Guddat, P. Gong, Z. Rao, Structural Basis for RNA Replication by the SARS-CoV-2 Polymerase, Cell 182 (2020) 417–428.e13, <https://doi.org/10.1016/j.cell.2020.05.034>.
- [39] E.P. Tchesnokov, J.Y. Feng, D.P. Porter, M. Götte, Mechanism of inhibition of Ebola virus RNA-dependent RNA polymerase by remdesivir, Viruses 11 (2019) 326, <https://doi.org/10.3390/v11040326>.
- [40] R.N. Kirchdoerfer, A.B. Ward, Structure of the SARS-CoV nsp12 polymerase bound to nsp7 and nsp8 co-factors, Nat. Commun. 10 (2019) 2342, <https://doi.org/10.1038/s41467-019-10280-3>.
- [41] L. Zhang, R. Zhou, Structural basis of the potential binding mechanism of remdesivir to SARS-CoV-2 RNA-dependent RNA polymerase, J. Phys. Chem. B 124 (2020) 6955–6962, <https://doi.org/10.1021/acs.jpcc.0c04198>.
- [42] I. Lucas-Gómez, A. López-Fernández, B.K. González-Pérez, M. Andrea, A.V. Calderón, M.A. Gayosso-Morales, Docking study for Protein Nsp-12 of SARS-CoV with Betalains and Alfa-Bisabolol, arXiv preprint arXiv (2020) 201214504.
- [43] Z. Elkarhat, H. Charoute, L. Elkhattabi, A. Barakat, H. Rouba, Potential inhibitors of SARS-cov-2 RNA dependent RNA polymerase protein: molecular docking, molecular dynamics simulations and MM-PBSA analyses, J. Biomol. Struct. Dyn. 40 (2022) 361–374, <https://doi.org/10.1080/07391102.2020.1813628>.
- [44] I. Celik, M. Erol, Z. Duzgun, In silico evaluation of potential inhibitory activity of remdesivir, favipiravir, ribavirin and galidesivir active forms on SARS-CoV-2 RNA polymerase, Mol Divers 26 (2022) 279–292, <https://doi.org/10.1007/s11030-021-10215-5>.
- [45] C.J. Rebello, R.A. Beyl, J.L. Lertora, H.F. Castro, S.R. Campagna, A.A. Coulter, L. M. Redman, F.L. Greenway, E. Ravussin, D.M. Ribnicki, A. Poulev, Safety and pharmacokinetics of naringenin: a randomized, controlled, single-ascending-dose clinical trial, Diabetes Obes. Metab. 22 (1) (2020) 91–98, <https://doi.org/10.1111/dom.13868>.
- [46] A.H.D. Cataneo, D. Kuczera, A.C. Koishi, C. Zanluca, G.F. Silveira, T.B.d. Arruda, A. A. Suzukawa, L.O. Bortot, M. Dias-Baruffi, W. Aparecido Verri Jr, A.W. Robert, M. A. Stimamiglio, C.N.D. dos Santos, P.F. Wovk, J. Bordignon, The citrus flavonoid naringenin impairs the in vitro infection of human cells by Zika virus, Sci. Rep. (2019) 16348, <https://doi.org/10.1038/s41598-019-52626-3>.
- [47] H. Huang, F. Sun, D.M. Owen, W. Li, Y. Chen, M. Gale Jr, J. Ye, Hepatitis C virus production by human hepatocytes dependent on assembly and secretion of very low-density lipoproteins, Proc. Natl. Acad. Sci. U. S. A. 104 (2007) 5848–5853, <https://doi.org/10.1073/pnas.0700760104>.
- [48] Y. Nahmias, J. Goldwasser, M. Casali, D. Van Poll, T. Wakita, R.T. Chung, M. L. Yarmush, Apolipoprotein B-dependent hepatitis C virus secretion is inhibited by the grapefruit flavonoid naringenin, Hepatology 47 (2008) 1437–1445, <https://doi.org/10.1002/hep.22197>.
- [49] J. Hodgson, ADMET-turning chemicals into drugs, Nat. Biotechnol. 19 (2001) 722–726, <https://doi.org/10.1038/90761>.
- [50] K. Wanat, Biological barriers, and the influence of protein binding on the passage of drugs across them, Mol. Biol. Rep. 47 (2020) 3221–3231, <https://doi.org/10.1007/s11033-020-05361-2>.
- [51] C.A. Lipinski, F. Lombardo, B.W. Dominy, P.J. Feeney, Experimental and computational approaches to estimate solubility and permeability in drug discovery and development settings, Adv. Drug. Deliv. Rev. 46 (2001) 3–26, [https://doi.org/10.1016/s0169-409x\(00\)00129-0](https://doi.org/10.1016/s0169-409x(00)00129-0).
- [52] J.L. Clark, P. Zahradka, C.G. Taylor, Efficacy of flavonoids in the management of high blood pressure, Nutr. Rev 73 (2015) 799–822, <https://doi.org/10.1093/nutr/nuv048>.
- [53] C. Dallas, A. Gerbi, Y. Elbez, P. Caillard, N. Zamaria, M. Cloarec, Clinical study to assess the efficacy and safety of a citrus polyphenolic extract of red Orange, grapefruit, and Orange (Sinetrol-XPur) on weight management and metabolic parameters in healthy overweight individuals, Phytother. Res. 28 (2014) 212–218, <https://doi.org/10.1002/ptr.4981>.
- [54] E. Hernández-Aquino, P. Muriel, Beneficial effects of naringenin in liver diseases: molecular mechanisms, World J. Gastroenterol. 24 (2018) 1679–1707, <https://doi.org/10.3748/wjg.v24.i16.1679>.
- [55] A. Salari-Jazi, K. Mahnam, P. Sadeghi, M.S. Damavandi, J. Faghri, Discovery of potential inhibitors against New Delhi metallo-β-lactamase-1 from natural compounds: in silico-based methods, Sci. Rep. 11 (2021) 2390, <https://doi.org/10.1038/s41598-021-82009-6>.
- [56] O. Trott, A.J. Olson, AutoDock Vina: improving the speed and accuracy of docking with a new scoring function, efficient optimization, and multithreading, J. Comput. Chem 31 (2010) 455–461, <https://doi.org/10.1002/jcc.21334>.
- [57] E.F. Pettersen, T.D. Goddard, C.C. Huang, G.S. Couch, D.M. Greenblatt, E.C. Meng, T.E. Ferrin, UCSF Chimera—a visualization system for exploratory research and analysis, J. Comput. Chem 25 (2004) 1605–1612, <https://doi.org/10.1002/jcc.20084>.
- [58] G.M. Morris, R. Huey, W. Lindstrom, M.F. Sanner, R.K. Belew, D.S. Goodsell, A. J. Olson, AutoDock4 and AutoDockTools4: automated docking with selective receptor flexibility, J. Comput. Chem. 30 (2009) 2785–2791, <https://doi.org/10.1002/jcc.21256>.

- [59] C. Honisch, M. Gazziero, R. Dallochio, A. Dessi, D. Fabbri, M.A. Dettori, G. Delogu, P. Ruzza, Antamanide Analogs as Potential Inhibitors of Tyrosinase, *Int. J. Mol. Sci.* 23 (2022) 6240, <https://doi.org/10.3390/ijms23116240>.
- [60] A.C. Wallace, R.A. Laskowski, J.M. Thornton, LIGPLOT: a program to generate schematic diagrams of protein-ligand interactions, *Protein Eng. Des. Sel* 8 (1995) 127–134, <https://doi.org/10.1093/protein/8.2.127>.
- [61] D. Van Der Spoel, E. Lindahl, B. Hess, G. Groenhof, A.E. Mark, H.J. Berendsen, GROMACS: fast, flexible, and free, *J. Comput. Chem.* 26 (2005) 1701–1718, <https://doi.org/10.1002/jcc.20291>.
- [62] A.W. Schüttelkopf, D.M. Van Aalten, PRODRG: a tool for high-throughput crystallography of protein-ligand complexes, *Acta. Crystallogr. D Biol. Crystallogr.* 60 (2004) 1355–1363, <https://doi.org/10.1107/S0907444904011679>.
- [63] A. Ali, R. Kumar, M.A. Iqbal, S. Jaiswal, D. Kumar, A.U. Khan, The role of conserved residues in catalytic activity of NDM-1: an approach of site directed mutagenesis and molecular dynamics, *Phys. Chem. Chem. Phys* 21 (2019) 17821–17835, <https://doi.org/10.1039/c9cp02734c>.
- [64] A. Daina, O. Michielin, V. Zoete, SwissADME: a free web tool to evaluate pharmacokinetics, drug-likeness and medicinal chemistry friendliness of small molecules, *Sci. Rep.* 7 (2017) 1–13, <https://doi.org/10.1038/srep42717>.
- [65] C.M. Ellison, J.C. Madden, M.T. Cronin, S.J. Enoch, Investigation of the Verhaar scheme for predicting acute aquatic toxicity: improving predictions obtained from Toxtree ver. 2.6, *Chemosphere* 139 (2015) 146–54, doi:10.1016/j.chemosphere.2015.06.009.